# INSTRUMENTATION

# Performance Evaluations of Recent Wide Field Scintillation Gamma Cameras

Chun Bin Lim, Paul B. Hoffer, F. David Rollo, and David L. Lilien

*University of California, San Francisco, California*

***Performance characteristics of four recent wide field scintillation gamma cameras were evaluated for 140-keV gamma imaging. Parameters measured included intrinsic spatial resolution, energy resolution, uniformity and linearity distortion, and count-rate capability and its influence on the spatial resolution. The system performance of the cameras was compared with representative parallel-channel collimators in terms of spatial resolution and relative sensitivity. Visual imaging comparisons of each camera system were performed by taking images of Rollo phantom containing four different lesion sizes, with four different contrast ratios, for equal imaging time.***

**J Nucl Med 19: 942–947, 1978**

The wide-field (15-inch or greater diameter) scintillation camera was developed by Anger in 1969 (*1*) and introduced commercially in 1975 (*2*). These devices have been accepted enthusiastically in the nuclear medicine community, and virtually all gamma camera manufacturers now produce them. Perhaps spurred by this competition, there has been progressive improvement in performance of the wide-field cameras in the past 2 years.

This paper reports the results of a comparison of the performance of the wide-field gamma cameras produced by three leading manufacturers, all of which were locally available for study. The manufacturers were given the opportunity to evaluate and adjust each camera before our study, and all of the cameras were performing at or near the manufacturer's specifications. Thus, though we only evaluated a single sample of each model, the results are felt to be typical of the performance of production units as of mid-1977. The gamma cameras included in this evaluation are listed in Table 1. The Ohio-Nuclear model 110 represents the initial production model of their wide-field camera, and it was re-evaluated after having been upgraded by the manufacturer to near equivalency with a later production model and is listed as model 410(1). A production model of the later version was also evaluated and is listed as model 410(2).

Basic design features of the cameras included in the study are shown in Table 2. A common feature is that they all use half-inch-thick NaI(Tl) crystals with 37 photomultiplier tubes (PMT). There are distinct differences in the light-pipe thickness, its preparation, the selection of PMT, and the associated electronics. For example, Searle's LFOV uses

**TABLE 1. CAMERAS USED FOR MEASUREMENT**

| Camera | Location* |
|---|---|
| 1. Searle LFOV | U.C. Medical Center |
| 2. Picker 4/15 | V.A. Hospital |
| 3. Ohio-Nuclear 110 | Franklin Hospital |
| 4. Ohio-Nuclear 410(1) | Franklin Hospital |
| 5. Ohio-Nuclear 410(2) | French Hospital |

* All in San Francisco.

Received Sept. 23, 1977; revision accepted Feb. 7, 1978.

For reprints contact: Chun Bin Lim, Nuclear Medicine Laboratory 455-S, University of California, San Francisco, CA 94143.

**TABLE 2. LARGE-FIELD DETECTOR SYSTEMS**

| | Searle LFOV | Picker 4/15 | Ohio Nuclear 110 and 410 |
|---|---|---|---|
| NaI(Tl) crystal thickness | ½ in. | ½ in. | ½ in. |
| Light-pipe thickness | 1⅛ in. | ½ in. | ¾ in. |
| PMT size and shape | 3 in. round | 3 in. hexagonal | 3 in. round |

**TABLE 3. DETECTOR PERFORMANCE COMPARISON**

| | | | (140 keV) Ohio-Nuclear | |
|---|---|---|---|---|
| | Searle-LFOV | Picker 4/15 | 110 | 410 (2)/ 410(1) |
| Intrinsic resolution (FWHM) | 6.5 mm | 4.7 mm | 6.5 mm | 4.5/ 5.5 mm |
| Max. count rate (20% window) | 145 K/s | 112 K/s | 92 K/s | 92 K/s |
| Count rate at 10% data loss | 70 K/s | 68 K/s | 68 K/s | 68 K/s |
| Energy resolution (FWHM) | 15% | 12% | 15% | 12/15% |

a light pipe 1⅛-in. thick that has V-shaped grooves around each conventional PMT of 3-in. diameter. One additional feature of this camera is the use of dc coupled electronics along the entire signal path from PMT outputs to the display oscilloscopes; this improves the camera's performance at high count rates. The Picker 4/15 uses hexagonal-shaped PMT so as to pack the crystal's area closely; these are coupled to a half-inch-thick, flat light pipe that has a special optical coating (snow-flake-shaped opaque coating) on its surface to correct for nonuniformity introduced by the thin light pipe. Ohio-Nuclear cameras use round PM tubes, 3-in. diameter and a ¾-in.-thick light pipe, in conjunction with nonlinear circuitry on the PMT outputs in the position channel to compensate for local nonuniformity. The ON-410(2), which was introduced early in 1977, uses newly introduced teacup PMT, which have improved photoelectron collection efficiency in the dynode stage (*3*). All cameras except ON-110 use some degree of thresholding on the PMT pulses in the position channel in order to improve the spatial resolution. To avoid degradation of energy resolution, however, they do not use thresholding in the energy channel.

## METHODS AND RESULTS

The following characteristics of each gamma camera were evaluated using the 140-keV photons of technetium-99m: a) intrinsic spatial resolution; b) linearity distortion and uniformity; c) count-rate capability and its influence on spatial resolution; d) energy resolution; and e) collimator system sensitivity and resolution. The results are summarized in Table 3 and the measurement methods and results are discussed below.

**Intrinsic spatial resolution.** This was measured by using PDP 11/40 computers interfaced to each camera. Intrinsic resolution was derived from line spread functions (LSF). The detector, uncollimated, was covered with a lead sheet 3/16-in. thick that had two 0.5-mm slits spaced 3 cm apart. A point source was placed, on axis, 1.5 m away. In the process of collecting data, the interface ADC gain was so adjusted that the two LSF images covered the 128 × 128 computer matrix frame. The two line slits were positioned near the middle of the detector. Full widths at half maximum (FWHM) from LSF were calculated by using the separation as scaling factor. The measured values on each camera are shown in

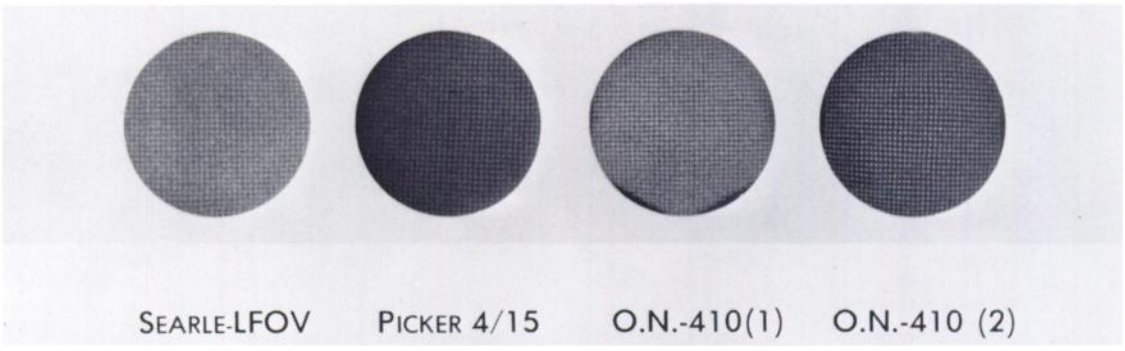


**FIG. 1.** Flood and linearity distortion (3/16-in. orthogonal hole pattern, 1 million counts each).

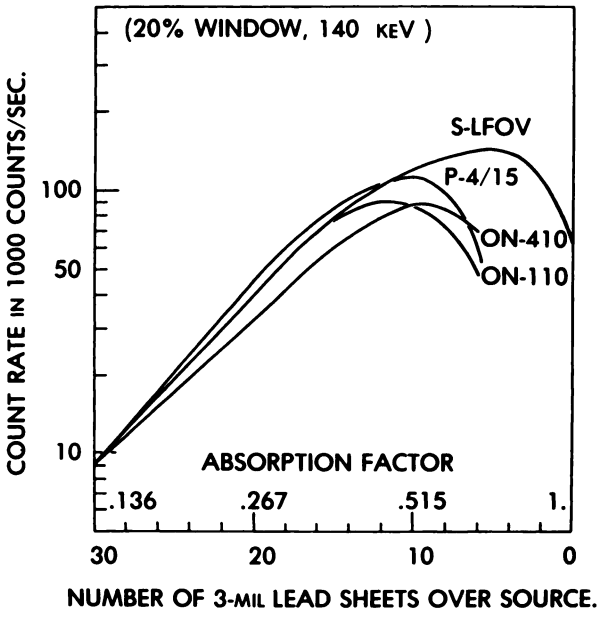


**FIG. 2.** Count-rate variation with source strength.

the first row of Table 3. The Picker 4/15 and ON-410(2) give about the same resolution capability—4.5 mm FWHM—compared with 6.5 mm FWHM for the Searle LFOV.

**Linearity distortion and uniformity.** Linearity distortion was measured using the Smith Orthogonal Hole Pattern (OHP) that has an orthogonal array of 3/16-in.-diameter holes with 3/8-in. between centers. The pattern images were obtained by exposing each detector, covered with an OHP pattern, to a point source 1.5 m away from the detector. The activity of the point source was adjusted to give 10,000 counts/sec in the detector and 1 million counts were collected for each picture. The pattern images are shown in Fig. 1. Subjective evaluation of linearity distortion revealed that the ON-410(1) and Searle LFOV performed best, whereas the Picker 4/15 and ON-410(2) showed some detectable distortion.

Uniformity was evaluated using the OHP pattern, and also with 1 million count flood images obtained under the same conditions except for removal of the OHP pattern. By visual inspection the uniformity appeared to be best on the ON-410(1), followed in order by the Searle LFOV, ON-410(2), and Picker 4/15. The ON-410(2) tended to show a pattern of a thick bar running in a 45° and 135° direction.

**Count-rate capability and its influence on resolution.** Count-rate performance with increasing photon flux was obtained by exposing each detector, uncollimated, to a Tc-99m source covered with a series of thin lead foils. The source was positioned approximately 1.5 m below the camera head and was put into a lead container in order to limit the photon exposure to the exposed detector area. The container was covered with 30 sheets of 0.003-in.

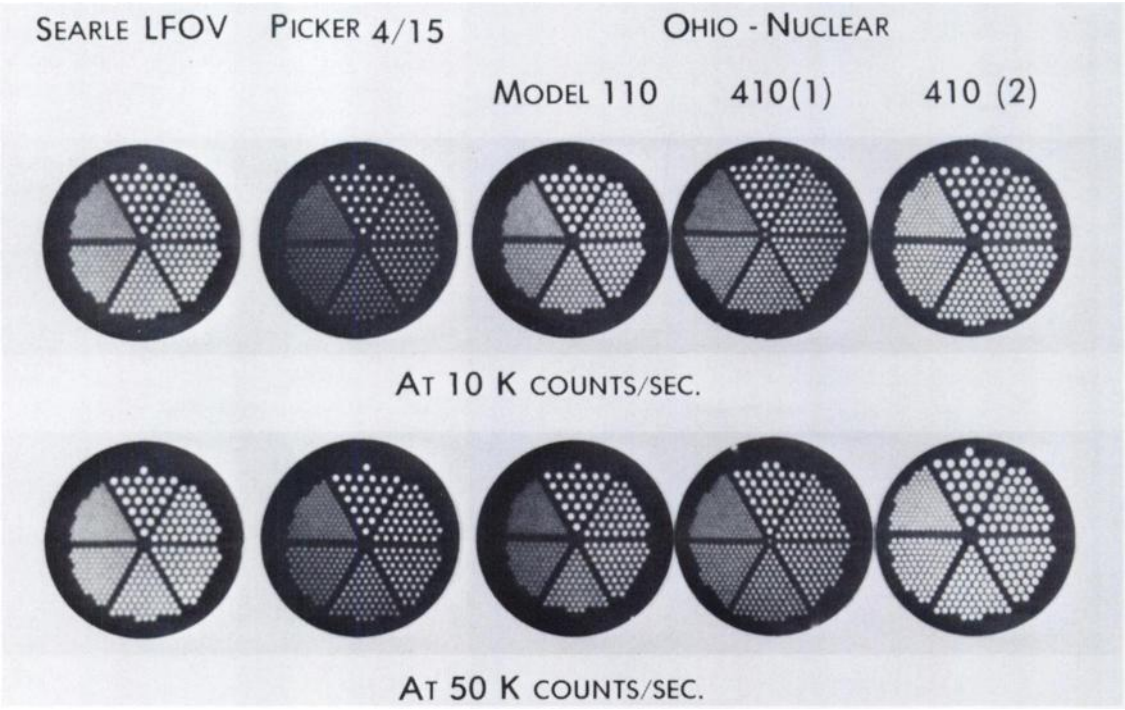


**FIG. 3.** Detector spatial resolution (Anger's pie pattern, 1 million counts each).

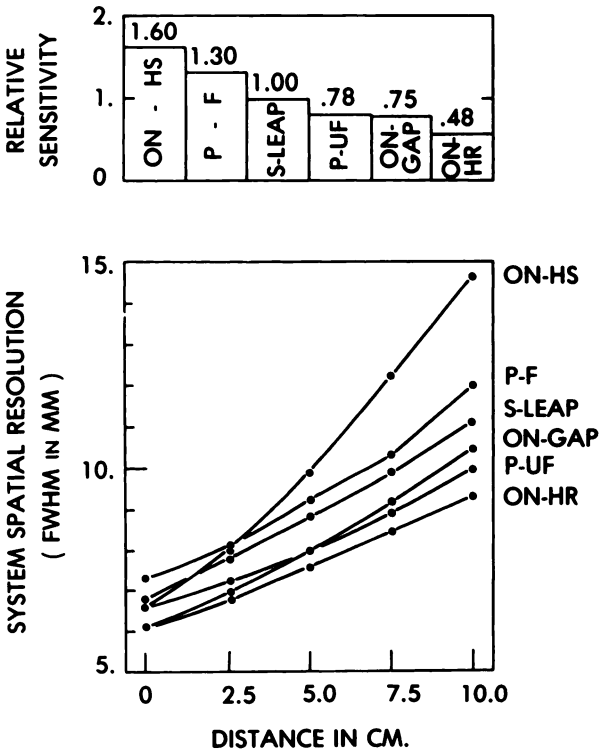


**FIG. 4.** Relative system sensitivity (top) and system spatial resolution (bottom) S = Searle LVOF; P = Picker 4/15; ON = Ohio-Nuclear 410. Collimators' LEAP = low-energy, all-purpose; F = fine; UF = ultra-fine; HR = high-resolution; GAP = general, all-purpose; HS = high-sensitivity.

lead foil that were removed two at a time between measurements to increase the exposure rate. The source was calibrated to give a count rate of 9,000/sec with a 20% energy window, centered over the peak, when 30 sheets were used. To ensure uniformity of measurement, the same lead foils were used for each camera under the same conditions. This measurement method, though convenient, has the drawback of introducing 80-keV lead X-rays that may add to the apparent dead time, especially at higher count rates. When results with this method were compared with those obtained using an uncovered source, the maximum observed decrease in count rate acceptance was 5–8%. However, since all cameras were evaluated by the same method, the relative results are valid though the curves would vary slightly from those shown (Fig. 2) if the results had been obtained using an uncovered source.

The count rates at 10% data loss, shown in the third row of Table 3, were obtained by extrapolating the count-rate curve at low exposure and reading the measured count rate at which the difference between the measured and extrapolated count rates is 10% of the extrapolated rate. The peak count-rate capability of the Searle LFOV was 145,000/sec against 100,000/sec for the Picker 4/15 and ON cameras.

The effects of count rate on spatial resolution were observed by using Anger's Pie Pattern (*4*). The pattern images taken at two count rates (10,000 and 50,000/sec) with each camera are shown in Fig. 3. Picker 4/15 and ON-410(2) resolve the 2 mm holes very clearly (as would be expected from 4.5 mm FWHM from LSF measurement), whereas the Searle LFOV barely resolves them. In all cameras tested, there was practically no noticeable degradation of resolution up to 50,000/sec, and only modest degradation up to approximately 80% of the peak count rate.

**Energy resolution.** This was measured at 140 keV by using the 93- and 185-keV peaks of Ga-67 for energy calibration of a 1024-channel multichannel analyser. Each camera was then exposed to a point source 1.5 m away from its uncollimated detector. Energy resolutions of the Picker 4/15 and ON-410(2) were 12% FWHM. Note that these two cameras also provide good spatial resolution, corroborating the physical expectation that the energy and spatial resolutions should improve together,

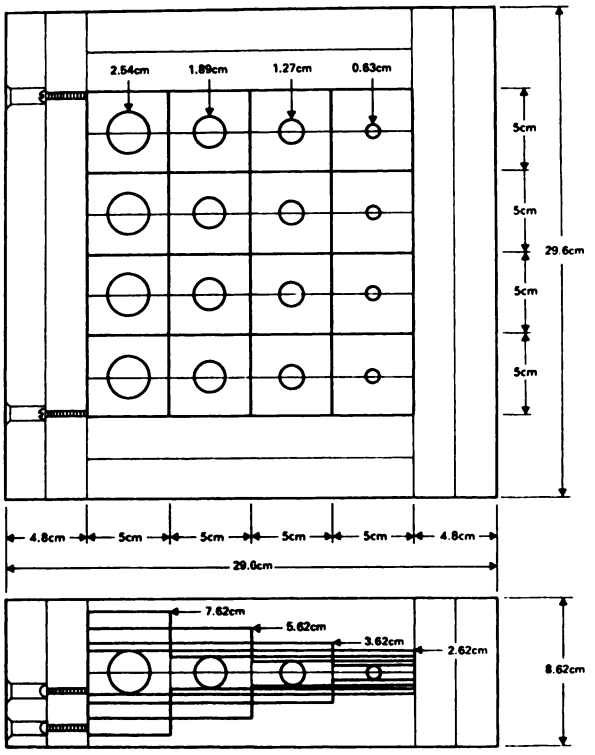


**FIG. 5.** Rollo Phantom: Constructed from Lucite; measures overall 29.6 × 29.6 × 8.62 cm; enclosing a hollow space that measures 20 × 20 × 7.62 cm; and contains 17 square interconnecting cells, each 5 cm on side. All cells can be filled with radioactive solution through two external ports. Each cell contains Lucite sphere centered within the cell such that all spheres appears within central plane of phantom. Thickness of each cell varies to provide each sphere with one of four different object contrasts: 0.66, 0.44, 0.33, and 0.22 cm (lower part of drawing).

since both are based on quantum collection statistics. All other cameras gave 15% FWHM energy resolution.

**Collimator system sensitivity and spatial resolution.** For the measurement of system performance the following combinations of imaging detectors and parallel-channel collimators were used: Searle (S) LFOV with low energy all purpose (LEAP) collimator, Picker (P) 4/15 with fine (F) and ultrafine (UF) collimators, and Ohio-Nuclear (ON) 410(1) with high resolution (HR), general all purpose (GAP) and high sensitivity (HS) collimators. The relative sensitivities of the camera systems was measured by exposing each camera to a circular flat flood source 25 cm in diameter and containing Tc-99m at the collimator face. These measurements were made successively on the same day with the time of measurement noted for each camera. The sensitivity readings were corrected for decay to compensate for the lapse of time. The results of the relative system sensitivities are shown in Fig. 4.

The spatial resolution of a system was evaluated in two ways: first, quantitatively by measuring the system LSF, and second, by phantom imaging and subjective visual inspection. The LSF measurement was performed by using two Tc-99m-filled parallel line sources of 0.5-mm inner diameter plastic tubing spaced 51 mm apart. LSFs from each camera were obtained at distances of 0 cm, 2.5 cm, 5.0 cm, 7.5 cm, and 10 cm from the collimator face. The FWHMs obtained from the LSFs are plotted in Fig. 4 for each camera system. No corrections were made for the actual diameter of the "line" source used. Examination of system spatial resolution behavior and relative sensitivity in Fig. 4 reveals, in general, a consistent trade-off between these two parameters in spite of the appreciable spread of the intrinsic resolution of the imaging detectors.

The subjective evaluation of actual imaging performance was performed using the Rollo phantom (Fig. 5), which has four different activity layers to provide four different contrasts. The phantom was filled with Tc-99m solution and imaged at distances of 0 cm, 2.5, 5.0, 7.5, and 10.0 cm from the collimator face. The Searle LFOV with LEAP collimator was arbitrarily used as a reference system by collecting 1 million counts and noting the time. Images with other camera/collimator combinations were

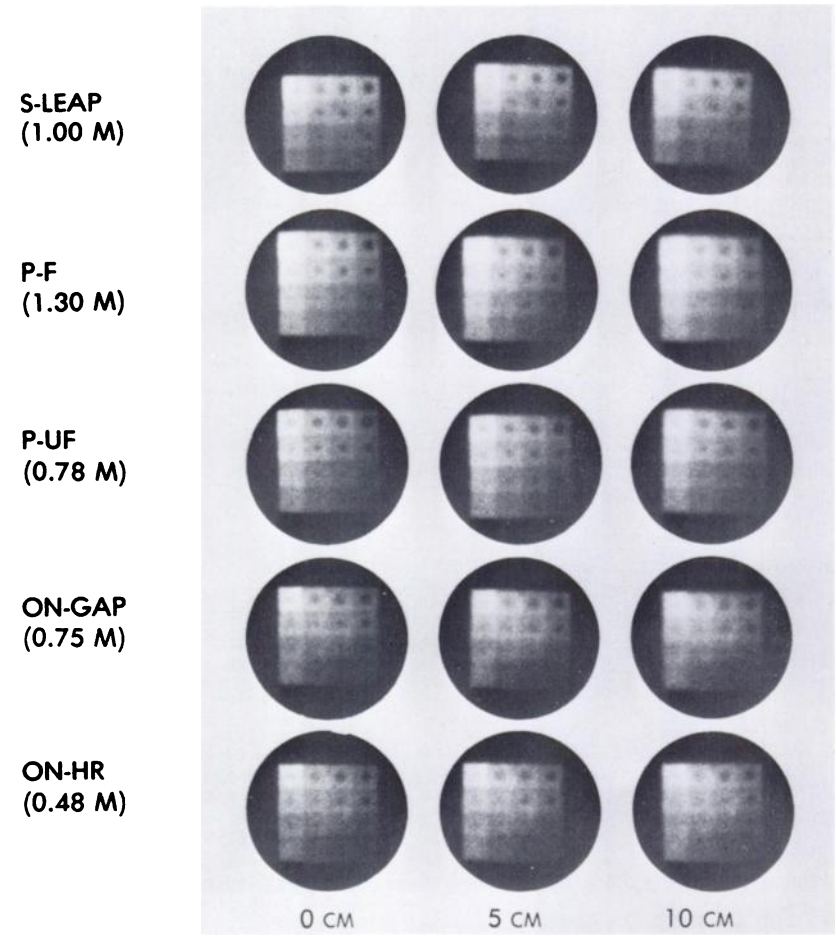


**FIG. 6.** Images of Rollo phantom at three distances from collimator face. Counting time equal for all.

obtained for the same time. The phantom images from five collimators at 5-cm steps are shown in Fig. 6. Except for the ON-HR images, which appear to show insufficient statistics due to lower collimator efficiency, careful inspection of these phantom images suggests little difference in resolution among the various systems.

## DISCUSSION

We have presented an evaluation of intrinsic and system imaging performances of the recent wide-field cameras of Searle, Picker, and Ohio-Nuclear. Two models, the Picker 4/15 and the ON-410(2), show distinct superiority in intrinsic spatial and energy resolution (4.5 mm FWHM and 12% FWHM, respectively). These improved resolution parameters, however, appear to have been achieved at the cost of increased susceptibility to nonuniformity and linearity distortions. One feature common to the two cameras is the use of light pipes thinner than that of Searle LFOV. The Searle LFOV had the best count rate capability—145,000/sec with 20% energy window.

Measurement of total system resolution and sensitivity revealed that the improvements in intrinsic resolution were not sufficient to disturb the basic trade-off between these two parameters in collimator design at system performance level. There was, however, a significant difference in selection of the optimal "routine" trade-off point between these two parameters among the camera manufacturers. When phantom imaging was performed to compare the actual imaging responses under equivalent imaging time, subjective evaluation of Rollo phantom images revealed little apparent resolution difference with equivalent scatter material thickness among similar collimators.

The primary purpose of this camera study was to measure the fundamental performance parameters of basic gamma camera imaging systems. We did not evaluate the possible alterations in performance when other instruments or peripherals are added to the basic system. The estimated basic performance can easily be affected when such accessories are added to a camera system.

Other factors related to long-term camera operation, such as the stability of operating characteristics and down-time frequency—which are important in terms of clinical operation—were not included in this evaluation. Potential buyers of cameras should also consider nontechnical aspects, such as local service support. These latter points may, in fact, be more important in camera selection than absolute system performance, since all the instruments tested performed very well.

## ACKNOWLEDGMENTS

We gratefully acknowledge the cooperation and assistance provided us by the three manufacturers whose products were evaluated. Specifically, we wish to thank Henry H. Wilson and John M. Fontius of Ohio-Nuclear, Inc., H. William Lollar of Searle, and Richard Sano and David Whitten of Picker.

This work was partially supported by ERDA Grant E(04-3)-34.

## REFERENCE

1. ANGER HO: Scintillation camera and multiplane tomographic scanner. *Japanese J Nucl Med* 6: 125–148, 1969

2. BURDINE JA, MURPHY PH: Clinical efficacy of a large-field-of-view scintillation camera. *J Nucl Med* 16: 1159–1165, 1975

3. ENGSTROM RW: Improvements in photomultiplier and TV camera tubes for nuclear medicine. *IEEE Trans Nucl Sci* NS-24, No. 2, 900–903, April 1977

4. ANGER HO: Testing the performance of scintillation cameras, LBL-2027, May 1973